Application of Regolith Polymer Composite Fused Granular Fabrication Construction in Simulated Lunar Conditions

Nathan J. Gelino[1], Evan A. Bell[2], David I. Malott[3], Steven E. Pfund[4], Matt W. Nugent[5], Marco A. Gudino[6]

[1]NASA, Kennedy Space Center, Exploration and Research Technology Programs, Swamp Works Kennedy Space Center, FL 32899; email: nathan.j.gelino@nasa.gov
[2]NASA, Kennedy Space Center, Exploration and Research Technology Programs, Swamp Works, Kennedy Space Center, FL 32899, email: evan.a.bell@nasa.gov
[3]SpaceFactory Inc., 901 Penhorn Ave Ste 1, Secaucus, NJ 07094; email: contact@spacefactory.ai
[4]LERA Consulting Structural Engineers RLLP, 40 Wall Street 23rd Floor, New York, NY 10005, email: stephen.pfund@lera.com
[5]Engineering Research and Consulting LLC, Kennedy Space Center, FL 32899, email: matthew.w.nugent@nasa.gov
[6]NASA, Kennedy Space Center, Exploration and Research Technology Programs, Swamp Works, Kennedy Space Center, FL 32899, email: marco.a.gudino@nasa.gov

ABSTRACT

NASA's Artemis program has the goal of creating a sustained lunar presence to provide unprecedented opportunities for scientific discovery and to ensure industry's access to the unlimited resources and commercial potential in space. To achieve this goal, NASA must incrementally develop and expand its capabilities beyond the short lunar stays of the Apollo program to a robust continued presence with infrastructure and equipment to reduce mission risk. Kennedy Space Center's Granular Mechanics and Regolith Operations laboratory (a.k.a. Swamp Works) has partnered with SpaceFactory and LERA Consulting Structural Engineers to develop the architectural and structural design of a robotically constructable unpressurized shelter. The shelter, called Lunar Infrastructure Asset (LINA), is designed to protect astronauts and surface assets from radiation, meteoroid impact, thermal gradients, and to withstand moonquakes. A Fused Granular Fabrication (FGF) construction process using regolith polymer composites was developed. The construction system and associated print parameters are discussed along with the environmental simulation equipment and a summary of test conditions. Test samples were printed in dirty thermal vacuum conditions (~10^{-3} torr, ~-200 °C,) and subscale versions of LINA were printed on a regolith simulant substrate in vacuum (~10^{-4} torr). Full scale LINA design optimization, simulation, and construction concept of operations are discussed.

INTRODUCTION

NASA's Artemis program has the goal of creating a sustained lunar presence to provide unprecedented opportunities for scientific discovery and to ensure industry's access to the unlimited resources and commercial potential in space. To achieve this goal, NASA must

incrementally develop and expand its capabilities beyond the short lunar stays of the Apollo program to a robust continued presence with infrastructure and equipment to reduce mission risk. Infrastructure can provide safer and more reliable access to the surface, its resources, and protection from the environment. Kennedy Space Center's Granular Mechanics and Regolith Operations laboratory (a.k.a. Swamp Works) has partnered with SpaceFactory and LERA Consulting Structural Engineers to develop the architectural and structural design of a robotically constructable unpressurized shelter. This work was completed under the Relevant Environment Additive Construction (REACT) project and in which a protective shelter, called Lunar Infrastructure Asset (LINA), is designed to protect astronauts and surface assets from radiation, meteoroid impact, thermal gradients, and to withstand moonquakes. An artistic rendering of LINA under construction on the moon is presented in Figure 1 (left). A Fused Granular Fabrication (FGF) construction process using regolith polymer composites was developed for simulated lunar conditions as an evolution of SpaceFactory's system that won the NASA 3D Printed Habitat Centennial Challenge (Figure 1 (right)) (Mueller 2019) and similar development activities at Swamp Works (Mueller 2018). The construction system, print parameters, environmental simulation equipment, and a summary of test conditions are discussed. Test samples were printed in simulated lunar dirty thermal vacuum conditions (~-200 °C, ~10^{-3} torr) and subjected to a series of characterization tests. The most relevant resulting properties are summarized here, the full details of the material characteristics are provided in a related paper (Gelino 2023-1). Subscale versions of LINA were printed on a regolith simulant substrate in vacuum (~10^{-4} torr) using a novel anchoring technique discussed below. LINA's structural design criteria and the resulting design are detailed in two papers that are pending publication (Sibille 2024) (Pfund 2024). Full scale LINA design optimization, simulation, and construction concept of operations are discussed.

Figure 1. An artistic rendering of LINA's full scale construction operations on the Moon (a). SpaceFactory wins the NASA 3D Printed Habitat Centennial Challenge (b).

TEST EQUIPMENT

Test samples were fabricated using the Advanced Regolith Ground Operations (ARGO) system made out of Regolith Polymer Composite (RPC). The system is outlined in detail in (Gelino 2023-2). A summary the ARGO system consists of the Atmospherically Sealed Simulator for In-situ System Testing (ASSIST) vacuum chamber, a 4-axis robotic gantry known as the ARGO gantry, cryogenic cold heads and shroud, a pellet extruder, a heated build plate, other robotic payloads, power supplies, regolith beds, and thermal and visible light cameras.

The testing outlined in this paper utilized the ASSIST chamber, ARGO gantry, the pellet extruder, heated build plate, cryogenic cold heads, cryo-shroud, and regolith beds. The configuration of the ARGO gantry in ASSIST with the heated bed and additive construction pellet extruder can be seen in Figure 2 (left).

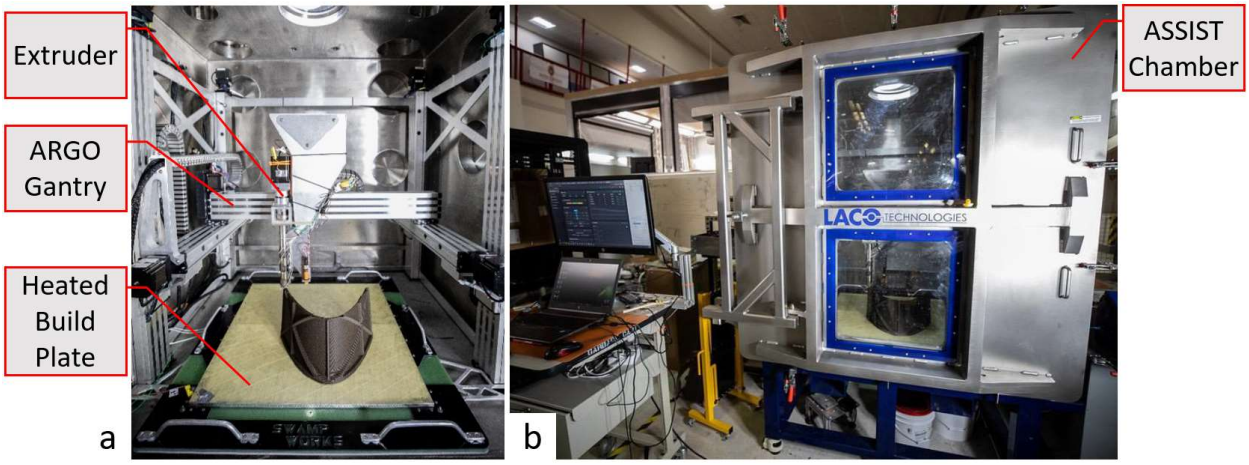

Figure 2. The ARGO gantry outfitted with pellet extruder is in the ASSIST chamber producing a LINA 1A prototype on the heated build plate (a). The ASSIST Chamber with active LINA construction operations under vacuum (b).

ASSIST Chamber. The ASSIST chamber is a dedicated Dirty Thermal Vacuum (DTVAC) chamber capable of pressure ranges between 760 torr (atmospheric) and 3.5×10^{-6} torr (high vacuum) (Gelino 2023-2). The chamber is 1.47 m x 1.47 m x 1.18 m and has a large front door (shown in Figure 2 (right)) allowing large test equipment, such as the ARGO gantry, to be installed without disassembly.

ARGO Gantry. The ARGO gantry is a 4-axis motion system designed for additive construction, as well as other manipulation tasks within a vacuum environment. The ASSIST chamber has reached 1×10^{-5} torr with the gantry installed. Lower pressures should be achievable given more pump-down time or the use of a cryogenic cooling device for cryo pumping the chamber. The gantry has a X, Y, Z, and E axis. The E axis was used to control the pellet extruder motor. Maximum gantry speed during testing was limited to 75 mm/s with a maximum build volume of 0.75 m x .75 m x 0.80 m and a positional accuracy of 0.033% of range and repeatability of 0.025 mm. The ARGO gantry system has an estimated mass of ~175 kg including the control system and pellet extruder.

The gantry and pellet extruder are driven by standard additive manufacturing G-Code commands. The system uses Klipper v0.11.0 open-source firmware (O'Connor 2022) on a Bigtreetech Octopus V1.4 control board. G-Code files were generated using the Ultimaker Cura slicer software (versions 5.0, 5.2, and 5.3). Manual control and upload of G-Code over a local area network was handled through a Raspberry Pi running Mainsail OS. Thermocouple inputs for the heaters and the heated build plate were converted to thermistor-like signals and read in by the Octopus board.

The pellet extruder, shown in Figure 3 (left), consists of a pellet feedstock hopper, a feed tube, an E-axis motor, a screw extruder with 3 closed loop heat zones, and a 3 mm diameter orifice extrusion nozzle. The feedstock hopper can contain up to 17 L of pellets. Each heater is independently controlled and can reach 250 °C. Heater 0 is used to both heat the lowest part of the screw extruder as well as thermally soak the nozzle. Typical extruded layer dimensions were 5.8 mm wide and 1.5 mm tall. During cryogenic testing, the heaters and screw extruder were thermally insulated to avoid radiative heating the cold shroud.

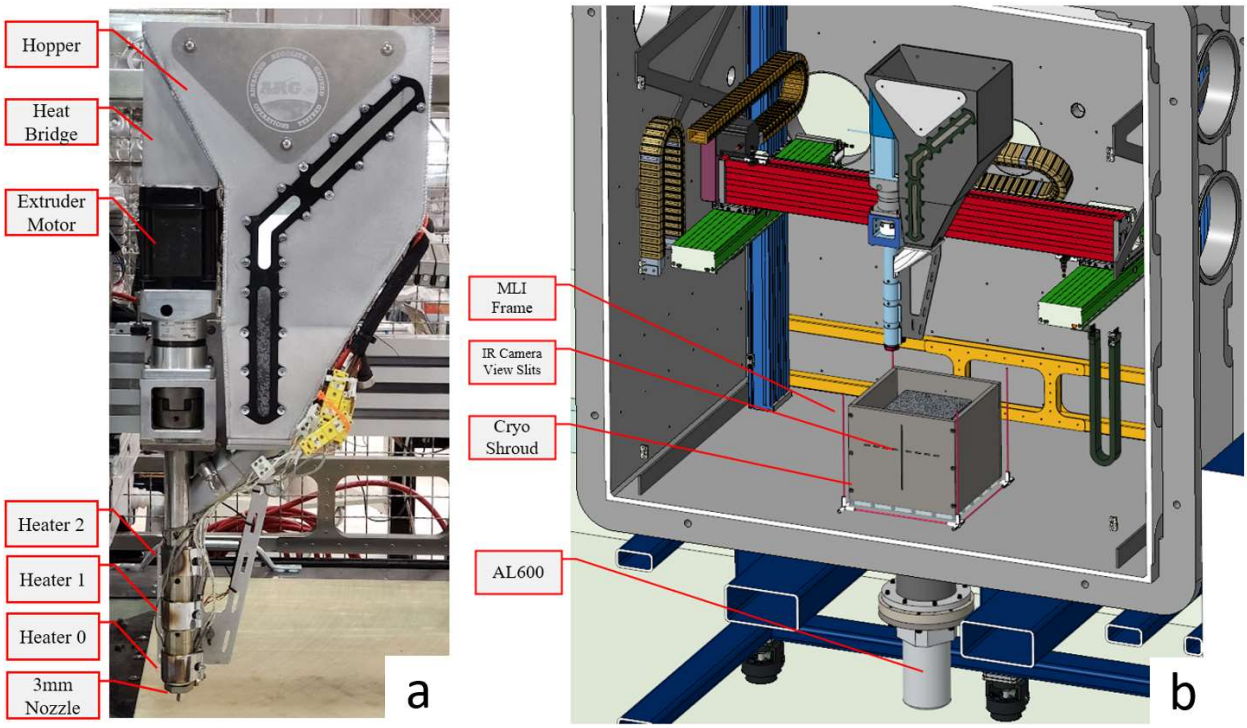

Figure 3. The RPC pellet extruder with heat zones use independent closed loop PID control in Klipper firmware and 17 L hopper (a). The cryo-shroud inside the ASSIST chamber with the AL600 cryocooler attached to the bottom of the cryo-shroud (b).

Maximum short-term extrusion rate was limited to 95 mm^3/s. If the system exceeds this speed or is operated at this speed for greater than ~2 minutes the screw extruder is unable to properly melt the polymer pellets and jams. Steady state extrusion was limited to 85 mm^3/s. In most cases, the flow rate of the extruder was limited by the desired travel speed times the cross section of the output bead, rather than by the limitations of the extruder system. The stepper motors

have a thermal operating limit of 100 °C before damage to the internal coil windings can occur. The E-axis stepper motor is in continual use during FGF construction, and it builds up heat quickly since convection is essentially non-existent in vacuum. Initially, there was a limit on total continuous print time of 8.3 hours to avoid over-heating. Subsequently, a convective heat path was made from the E motor through a heat bridge to the hopper with a 5 lb. copper disk heat sink attached. The extruder could run indefinitely after the modification.

The tool zero position was found either by manually probing the bed or using a BL Touch probe sensor (not shown) to perform 9-point bed mesh leveling in Klipper. The BL touch was used for final LINA construction. Manual leveling was used during cryogenic testing.

Cryo-Shroud. A Cryomech AL600 cryocooler was used for cryogenic testing along with a custom aluminum shroud to simulate radiation heat loss from the test specimen to the black body absorption of space. The configuration of the shroud within the ASSIST chamber is shown above in Figure 3 (right). The AL600 cryocooler was mounted to the underside of the chamber using an ISO160F flange. Six fasteners were used to attach the shroud to the cryocooler's copper cold block which protrudes into the chamber. Thermal paste was used between the two surfaces to reduce thermal contact resistance. Thermal data was gathered through view slits on the cryo-shroud facing the front door IR viewport with a FLIR A35 FOV45. Multi-layer insulation (MLI) was wrapped onto a frame and placed around the cryo-shroud to reduce radiative heating of the cryo-shroud from the gantry and ASSIST's walls.

Figure 4 shows the cryo-shroud and build plate assembly. The build plate was made of Polylactic Acid (PLA) and was a consumable item that was replaced after each test. It was fastened to a G10 substrate plate to provide thermal insulation as well as easy attachment to the cryo-shroud. The G10 plate used internally threaded G10 standoffs as a conductive heat break between the G10 plate and the cryo-shroud. Five MLI sheets were placed between cryo-shroud and the G10 substrate to act as a radiative barrier to the build plate. Square tube printed RPC samples were constructed on top of the PLA build plates and could be viewed through the IR view slits.

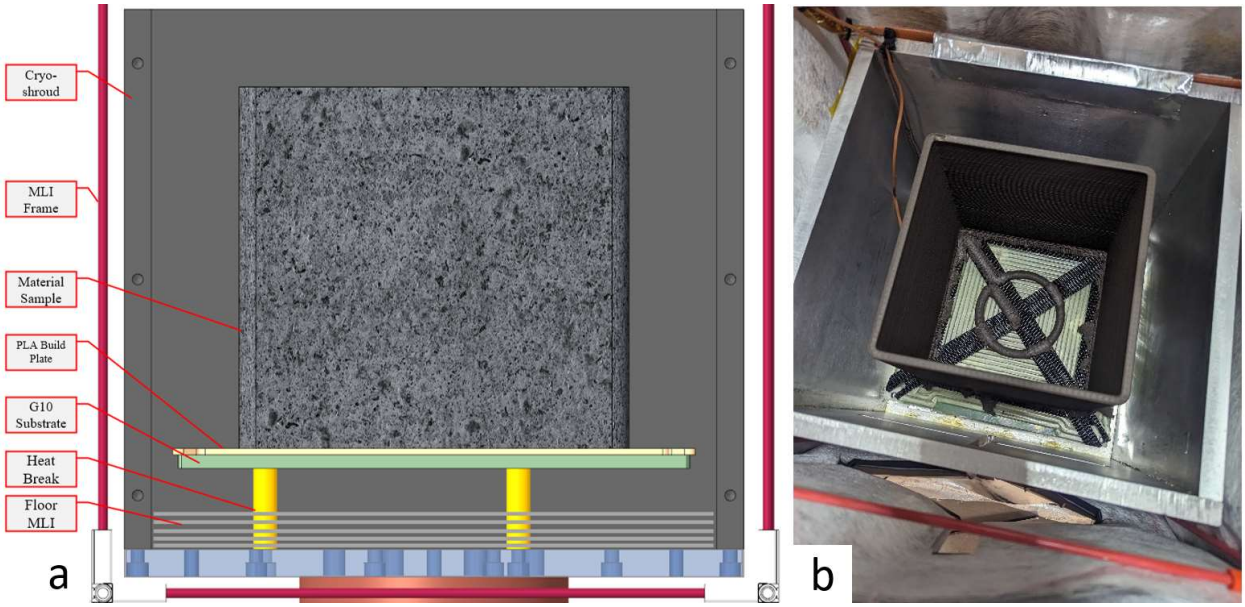

Figure 4. The cryo-shroud assembly with printed RPC tube and MLI frame. Side view of CAD (a). Top view of in-ASSIST assembly with printed material sample (b).

Figure 5 (a) shows the location of three E-type Thermocouples (TC) that were used to measure the temperature of the cryo-shroud. The wall TCs were clamped to the backside (the side facing away from the printed RPC sample) using #10-32 flat head screws. The conical head of the fastener was used to press the TC into the shroud firmly. The AL600 contact TC was attached using one of the 6 fasteners of the cold head and clamped to the cryo-shroud surface using a copper washer (Figure 5(b)). Belleville spring washers were used to apply consistent clamping load even if differences in the coefficient of thermal expansion between the shroud and the bolt reduced the bolted connection's tension. This happened when not using the spring washers and reduced cooling rate significantly.

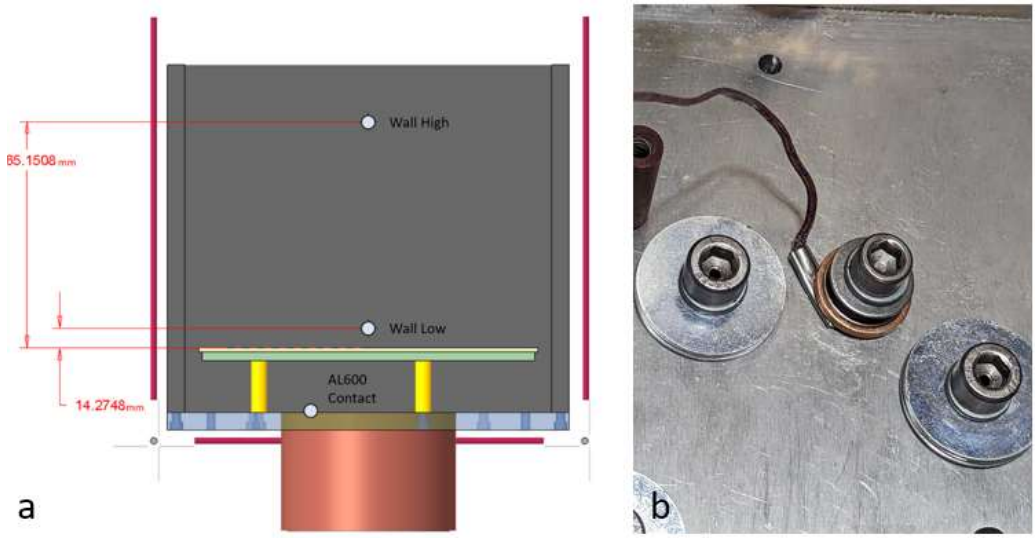

Figure 5. Two E-type thermocouples are positioned along the back wall of the cryo-shroud (a). The AL600 contact TC is clamped to the cryo-shroud (b).

The wall high TC consistently read warmer than wall low and AL600 contact TCs. Similarly, wall low TC consistently read warmer than AL600 contact TC. The typical cooling rates are shown in Figure 6. An additional K-type thermocouple was clamped to the PLA build plate to measure the temperature. This was consistently the warmest temperature of the four at -90 to -100 °C during testing. This temperature was low enough that the first layer of the RPC sample tube was unable to adhere to the PLA build plate. Adhesion to the build plate was achieved using a mechanical locking barb that is outlined in the Subscale Lina Construction section of the paper.

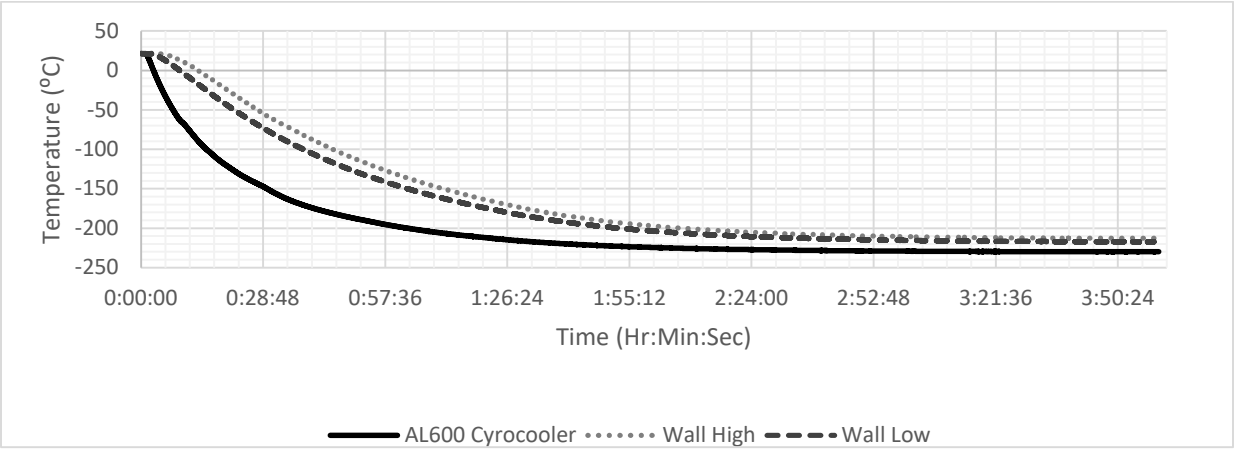

Figure 6. The typical cryo-shroud cooling rate using the AL600 cryocooler.

ADDITIVE CONSTRUCTION TESTING

Initial Feasibility Testing. Regolith Polymer Composite (RPC) formulations were developed and evaluated for suitability for additive construction in simulated lunar vacuum and thermal conditions by printing sample geometry and testing the materials.

A summary of the RPC production process is provided below, a detailed description can be found in (Gelino 2023-1). RPC materials were prepared by mixing dried polymer binders and regolith simulants in a compounding process. The process feeds each material into an extruder at controlled rates to produce the desired mixture ratios. A filament is extruded, cooled in a water bath, and chopped into pellets. The pellets are dried placed in the ARGO hopper as additive construction feedstock. Eight formulations were evaluated using Black Point-1 (BP-1) and Lunar Highlands Simulant-1 (LHS-1) simulants along with Polypropylene (PP) and Polylactic Acid (PLA) binders. The first four formulations in Table 1 were printed at ~10^{-3} torr and ambient temperature to assess basic feasibility of additive construction in vacuum.

The printing process is shown in Figure **7** (a) along with initial porosity issues with PP based formulations (b) but not with PLA based formulations (c). The remaining formulations in Table 1 were printed into square tubes beginning at ~10^{-3} torr and ~-200 °C (not steady state). The TVAC additive construction and the resulting RPC test cubes are show in Figure 8. The tubes were cut into panels, water jetted into test pieces, and tested for various characteristics. Ultimate flexural strength and flexural modulus control LINA's structural design and are shown in Table 1.

Table 1. Seven RPC formulations were additively constructed in simulated lunar TVAC and evaluated for strength properties and other characteristics.

Formulation	Target Mixture Ratio (wt%)	Significant Porosity Observed?	Average Ultimate Flexural Strength (MPa)***	Average Flexural Modulus of Elasticity (GPa)***
BP-1: PP: Additive*	50: 48: 2	Yes	N/A	N/A
BP-1: PP	50: 50	Yes	N/A	N/A
PP-1: PLA	50: 50	No	N/A	N/A
BP-1: PLA	70: 30	No	17.5	1.93
BP-1: PLA	80: 20	No	17.7	2.87
BP-1: PLA: Additive**	80: 18.5: 1.5	No	18.2	3.13
LHS-1: PLA	80: 20	No	16.5	3.65
BP-1: PLA	85: 15	No	12.5	2.63

* SCONA TPPP 9212 GA compatibilizer, 1.8% wt% maleic anhydride grafted to PP
**ST-PA210 flow enhancer, consumed during compounding process
***Force loading orientation is perpendicular to the grain (worst case)

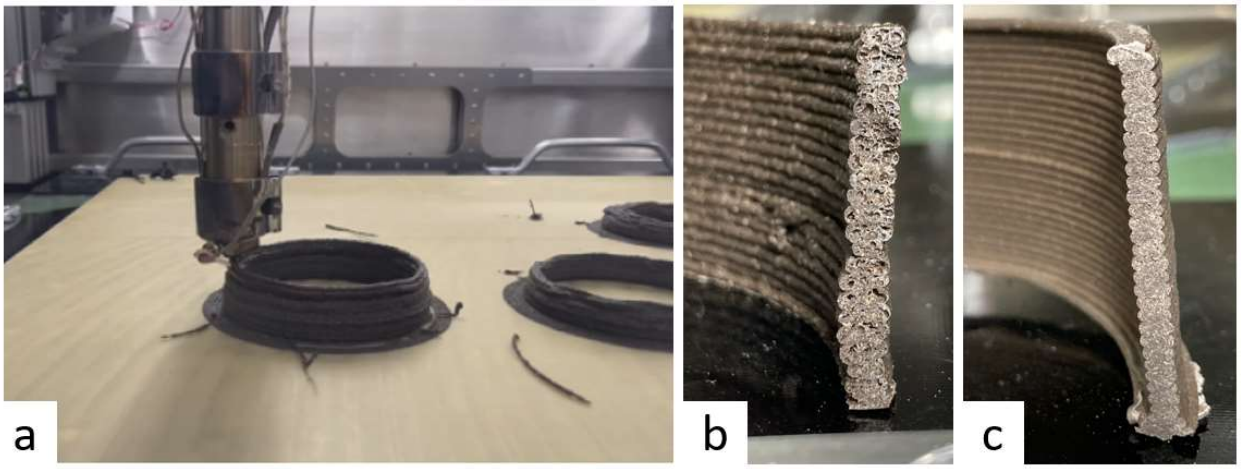

Figure 7. Basic feasibility of RPC construction is proven in vacuum (a). Significant porosity was observed in PP formulations (b) but not in PLA formulations (c).

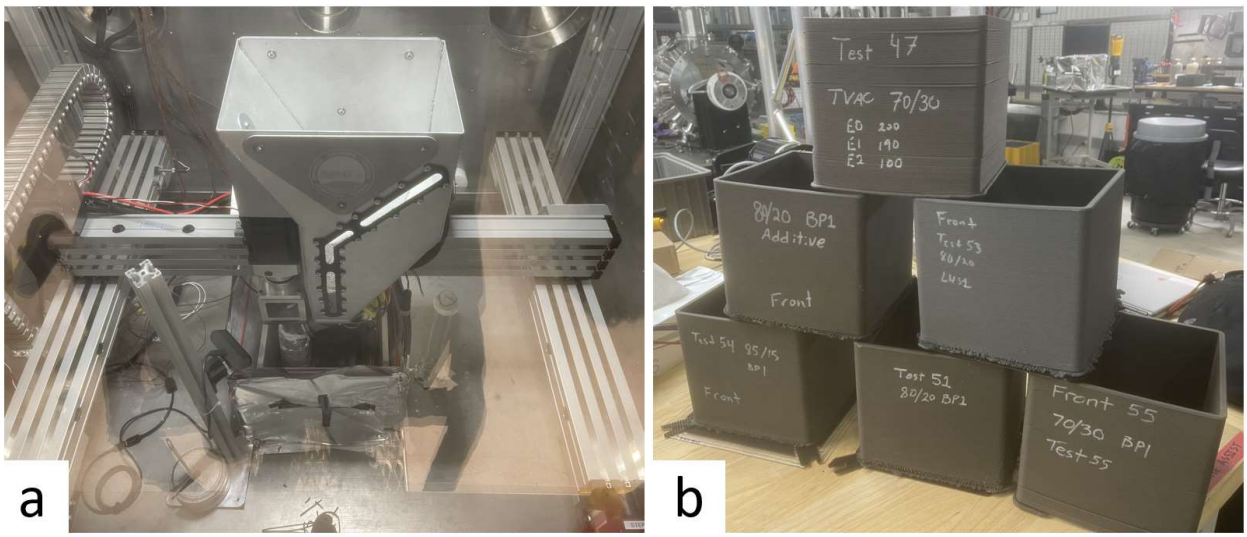

Figure 8. Test samples are printed in TVAC (a) and displayed (b).

Energy Consumption. Energy consumption was measured for each of the Beta formulation test prints using two watt meters (KW46-US Electricity Usage Monitor) located at the 110V facility power outlets that supply the system. Energy consumption was recorded separately for the extruder heaters and the stepper motors (including the overall control system) and reported in Table 2 along with the steady state nozzle temperature. The average energy consumption for the full construction system per printed volume was ~3 MWh/m^3.

Table 2. Energy consumption and steady state nozzle temperatures for each formulation.

Formulation	Heater Energy (kWh)	Stepper Energy (kWh)	Nozzle Steady State Temperature (°C)
BP-1: PLA, 70: 30	0.08	1.920	181.8
BP-1: PLA, 80:20	0.045	1.943	182.7
BP-1: PLA: Additive, 80: 18.5: 1.5	0.046	1.979	182.5
LHS-1: PLA, 80: 20	0.031	2.033	188.1
BP-1: PLA, 85: 15	0.08	1.894	186.25

Subscale LINA Construction. Two permutations of LINA structure were successfully constructed in vacuum conditions. Figure 9 (a) and (b) show the LINA 2A which utilizes a ribbed structure for support while (c) and (d) show a corrugated design that maintains strength while optimizing the design for FGF construction. Both designs utilized the custom Cura parameters outlined in APPENDIX A: CUSTOM CURA SETTINGS. LINA was built on both medium-density fiberboard (MDF) and on an LHS-1 simulant substrate. The MDF board was used for early construction testing to simulate the insulative effects of regolith and the lack of adhesion of layers to the MDF acted like a powder regolith simulant build surface. Construction tests on regolith simulant used a ~2mm thick layer of LHS-1 on top of MDF as a build surface.

The FGF construction article was unable to adhere to the LHS-1 surface despite numerous attempts using several securing approaches. An anchoring system was developed to prevent part movement or warping during construction (Figure 10). The anchoring system utilized snap-together fastener strips (commonly referred as 3M brand dual-lock) mounted to the MDF board using screws. The first layer of the structure "connected the dots" across the anchors and was set to "over extrude" to flow into, under, and around the individual locking elements of the anchors. This provided a mechanical connection to the bed and simulated a lunar construction concept in which ground anchors with locking features on top are prepositioned along the print path. The test anchors were 12mm wide and 2mm tall. The z offset of the extruder was set to cause the 0.5 to 1.5 mm of extruded material to flow into the anchors. The anchor spacing equated to 2m at full scale. It is anticipated that a large increase in spacing is possible, therefor reducing the number of anchors required.

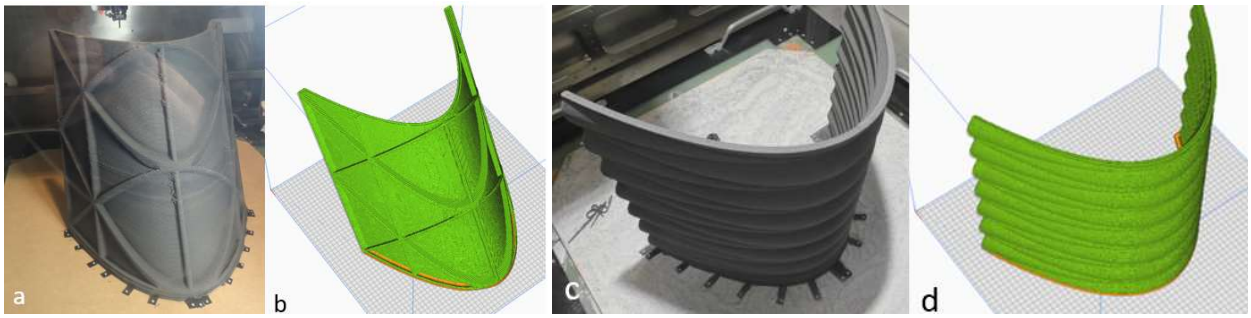

Figure 9. The LINA 2A completed print in vacuum on MDF board (a). Cura slicer preview of LINA 2A (b). The LINA 2B completed print in vacuum on LHS-1 simulant (c). Cura slicer preview of LINA 2B (d).

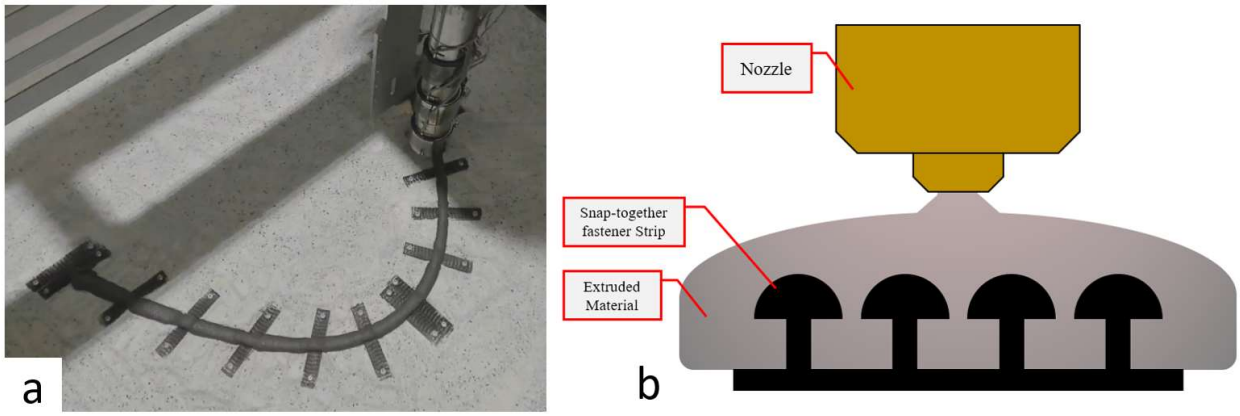

Figure 10. LINA 2B's first layer is over-extruded to fill in the mechanical interlocks on the anchor system (a). Extruded material flows into and around the anchor features (b).

The LINA structures took approximately 8 hours and 50 minutes to build. The PID control loops for each heater were set to the following: heater 0: 200 °C, heater 1: 200 °C, heater 2: 0 °C. During operation, a significant amount of heat is produced within the barrel of the extruder due to shear friction forces. This friction maintains the temperature within the barrel with only minor heat input from the heaters. During steady state operation, temperatures at each heater and the nozzle

were recorded to be approximately 217 °C for heater 0, 207 °C for heater 1, 119 °C for heater 2, and 197 °C for the nozzle.

The lowest pressure during LINA construction was $3.2x10^{-4}$ torr at the start of construction as shown in Figure 11. During construction the pressure steadily increased to a peak and then began to go back down. It is likely the first layers of the printing process bakes out the LHS-1 substrate and MDF causing the pressure increase. A similar pressure increase can be seen when pre-heating the barrel which likely causes volatilization material in the barrel and other residues.

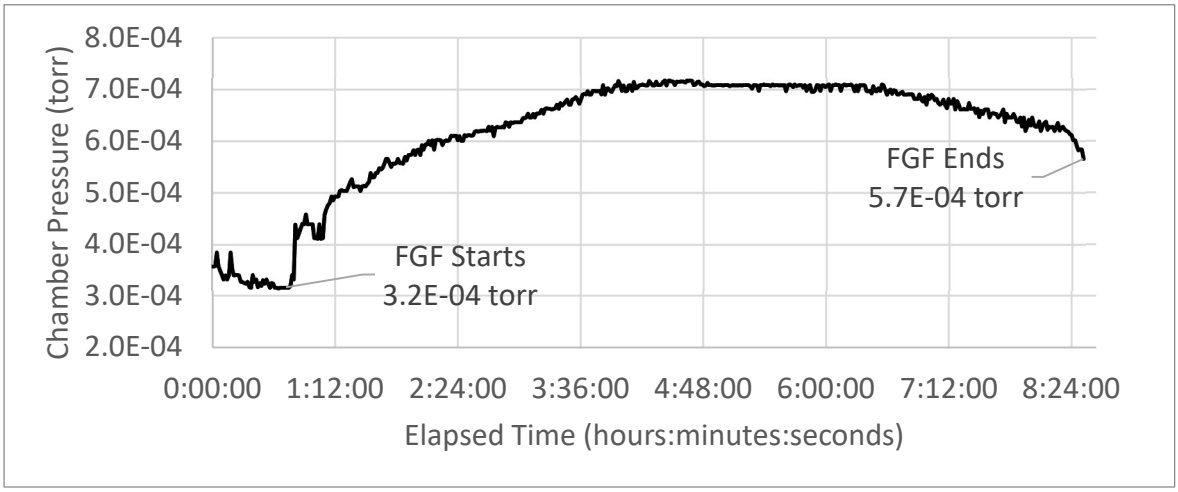

Figure 11. Pressure within ASSIST during LINA FGF construction.

FULL SCALE LINA CONSTRUCTION CONSIDERATIONS

Architectural and Structural Optimization. Flexural modulus significantly exceeded the initial assumed value used in the LINA 2A design, which was conservatively based on the preliminary tests results with cross-layer (90-degree) test samples. Additionally, the approach of inclined 3D printing, with layer lines oriented approximately 45-degrees relative to the ground (as seen in Figure 1), suggested the feasibility of averaging the in-layer (0-degree) and cross-layer (90-degree) test sample properties for use in the LINA 2B structural design.

Furthermore, observations of partial delamination at the intersections of the printed LINA 2A diagrid and slumping of the spanning shell between the diagrid and at unsupported overhangs prompted the proposition of a corrugated version, termed LINA 2B. This modification aimed to enhance the 'printability' of the structure by mitigating the aforementioned delamination and slumping and to enhance the structural performance using an increased flexural modulus based on the testing program and averaging the results from in-layer and cross-layer material properties.

Overall, in comparison to the original LINA 2A diagrid design, the updated LINA 2B corrugated design with enhanced material properties resulted in a reduction to the required full scale shell thickness from 50mm to 30mm, a reduced average structural cross-section depth, and a total mass reduction of approximately 40%. Such reductions not only minimized the printing duration but also decreased the up-mass of any imported binder material, thereby improving the construction process viability.

Full Scale LINA Simulation. The DTVAC test results informed the development of a thermal analysis software by SpaceFactory. Calibrated with thermal imaging data from ARGO's FLIR camera, the thermal simulation factored both radiative heat transfer and conduction within the print. Ground conductivity was ignored due to the low thermal conductivity of the regolith.

The software was designed to interpret G-Code from actual printing processes and extrapolate it to full scale. Assumptions were made to establish bounds for print velocity (mm/s) and throughput (mm^3/sec) pertinent to a full-scale lunar surface additive construction system. A key simulation goal was to emulate the layer-to-layer cooling rate of the test square tubes, which demonstrated optimal structural properties. This suggests that replicating the subscale cooling rates in a full-scale 3D print can potentially increase the likelihood of a successful lunar surface print.

Multiple iterations using the software indicated a throughput of 50 kg/hr. Given thermal conditions averaging -200°C (sky exposure) and -100°C (ground exposure), the estimated print time for a full-scale LINA was 11.6 days. Future analyses will incorporate lunar daylight temperature variations and potential self-shading of the structure, which might introduce variable temperature regions within the print.

Preliminary Concept of Operations. Given LINA's vaulted geometry, conventional horizontal layer printing was deemed unsuitable. Implementing such a method would lead to bridging challenges at the vault's apex, necessitating the addition of temporary support structures. To sidestep this complexity, our focus gravitated towards two primary methodologies:

1. Tilt-up Construction: This technique would involve the printing of approximately 1-meter tall vault segments directly on the lunar surface. Once printed, these segments would be erected or "tilted-up" into their desired position. A salient feature of this method would be the incorporation of interlocking designs printed into each segment, ensuring structural coherence when assembled. Other assembly methods could be used such as tensioned cable ties.
2. Inclined Angle Printing: Here, the structure would be printed at an inclined angle ranging between 30 to 45 degrees. This would necessitate a modification to LINA's posterior design, ensuring it firmly establishes contact with the ground. This base or "starter block" would provide a foundation, from which the vaulted design can progressively be printed outward. A significant advantage of this approach is its continuity, offering a structurally coherent print that simultaneously obviates the need for post-print assembly.

The latter approach was adopted and demonstrated by slicing the subscale LINA 2A and 2B models at 60-degree and 90-degree angles, respectively.

CONCLUSIONS

NASA's Artemis program has the goal of creating a sustained lunar presence to enable a vibrant cislunar economy and to enhance science exploration. Developing lunar construction capabilities is an important step towards realizing these objectives. Infrastructure on the Moon will reduce overall mission risks by providing access to power, improved reliability of transportation to and across the surface, and enabling exchange of commodities and services in-situ among other things.

Infrastructure like LINA can provide for one of humanities' most basic needs: protection from the environment.

This project demonstrated the use of FGF construction processes and materials in simulated lunar environments and yielded high quality subscale versions of a protective shelter (Figure 12). The design of the shelter was engineered based on the best available lunar environmental dataFigure 11. The FGF additive construction systems, processes, and materials described in this paper are approaching Technology Readiness Level (TRL) 5. This assessment is based on: (1) the successful completion of additive construction processes in simulated lunar environmental conditions where test articles were printed in DTVAC with simultaneous pressures and temperatures as low as 10^{-3} torr and -200 °C respectfully. (2) The resultant materials were characterized in ambient conditions to yield properties suitable for structural applications. (3) LINA, an engineered subscale protective shelter with complex geometry, was printed at 10^{-4} torr on a regolith simulant substrate. (4) Construction of full-scale structures was demonstrated during the NASA 3D Printed Habitat Centennial Challenge.

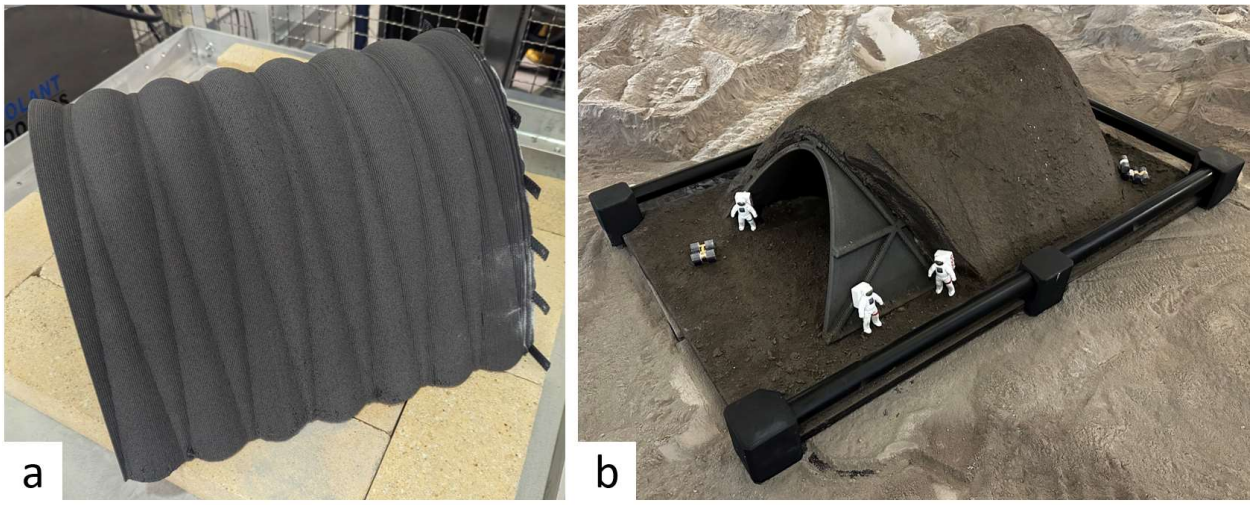

Figure 12. Vacuum construction of LINA 2B yields a high-quality subscale structure (a). LINA 1B is incorporated into a model showing the shelter in use on the Moon (b).

Additional development is required to reach full TRL 5 including designing the extrusion and positioning systems for flight rather than ground testing; evaluating the systems and materials across their entire expected thermal range as opposed to only cooling the build volume and testing material properties in ambient conditions respectively; assessing the material's performance across the expected life of the facility; mitigating dust exposure; feedstock handling, and numerous others. Though LINA has been designed for this construction process using design criteria based on the best available lunar environmental information and commercial terrestrial structural design validation techniques, much work remains before any such structure could be considered for construction and certified for human occupancy on the Moon.

APPENDIX A: CUSTOM CURA SETTINGS

Setting	Value	Units
Layer Height	1.5	mm
Initial Layer Height	4.0	mm
Line Width	4.0	mm
Initial Layer Line Width	250	%
Top/Bottom Thickness	0.0	mm
Infill Density	0	%
Print Speed	12.0	Mm/s
Wall Speed	12.0	Mm/s
Travel Speed	25.0	Mm/s
Initial Layer Print Speed	2.0	Mm/s
Flow Equalization Ratio	100	%
Build Plate Adhesion Type	Raft	Dropdown Selection
Raft Extra Margin	0.0	mm
Raft Smoothing	0.0	mm
Raft Base Line Width	10.0	mm
Raft Print Speed	1.6	mm /s
Merged Meshes Overlap	0.15	Mm
Spiralize Out Contour	Yes	Checkbox
Smooth Spiralized Contours	Yes	Checkbox
Slicing Tolerance	Middle	Dropdown Selection

Printer Configuration Setting	Value	Unit
Printer X/Y/Z Size	550/550/550	mm/mm/mm/
Nozzle Size	3.0	mm
Compatible Material Diameter	2.85	Mm

REFERENCES

Mueller, R. P., Prater, T. J., Roman, M., Edmunson, J. E., Fiske, M. R., & Carrato, P. (2019, October). NASA centennial challenge: three dimensional (3D) printed habitat, phase 3. In 70th International Astronautical Congress (IAC) (No. KSC-E-DAA-TN74064).

Mueller, R. P., Gelino, N. J., Smith, J. D., Buckles, B. C., Lippitt, T., Schuler, J. M., ... & Townsend, I. I. (2018, April). Zero launch mass three-dimensional print head. In 16th Biennial International Conference on Engineering, Science, Construction, and Operations in Challenging Environments (pp. 219-232). Reston, VA: American Society of Civil Engineers.

Gelino, N. J., Smith, J. L., Irwin, T. D., Lipscomb, T. A., Bell, E. A., Malott, D. I., Pfund, S. J., Herrera, L. H., Gomes, C. G., Gibson, T. L., Hwang, J. Z., McLeod, C. J., Sibille, L., Gudino, M. A. (2024, March). "Selection, Production, and Properties of Regolith Polymer Composites for Lunar Construction." IEEE Aerospace Conference, Big Sky, MT.

Sibille, L., Gelino, N. J., Pfund, S., J., McCarthy, A., Malott, D. I. (2024). "Development of lunar structural design criteria using terrestrial design practices and interpreted lunar conditions," J. Aerosp. Eng., Manuscript in Preparation.

Pfund, S. J., Malott, D. I., McCarthy, A., Cornelius, B., Sibille, L., Gelino, N. J., (2024) "Building on the Moon- Methods for Structural Validation and Architectural Design Implications," *J. Aerosp. Eng.*, Manuscript in Preparation.

Gelino, Nathan J., Bell, Evan A., Nugent, Matthew W., (in review, 2023-2). "Development of the Advanced Regolith Ground Operations (ARGO) Test Bed – A Robotic Excavation and Construction Test Facility with Simulated Lunar Environments." ASCEND Conference, Las Vegas, NV.

O'Connor, K., Callahan, E. (2022). Klipper firmware (Version 0.11.0). [Firmware]. https://www.klipper3d.org.